Published by :
http://www.ijert.org

International Journal of Engineering Research & Technology (IJERT)
ISSN: 2278-0181
Vol. 5 Issue 06, June-2016

Experimental Study of Fluid Flow and Heat Transfer Characteristics of Rough Surface, Impinged by a Confined Laminar Slot Air Jet

M. Adimurthy[1], ,
[1]Associate professor,
Department of Automobile Engineering,
BLDEA's DR. PGH CET, Vijayapura,
Karnataka, 586103

Venkatesha[2]
[2]PG Student,
Thermal Power Engineering,
Department of Mechanical Engineering,
BLDEA's DR. PGH CET,
Vijayapura, Karnataka, 586103,

Vadiraj V Katti[3]
[3]Principal. KLS VDRIT,
Haliyal, Uttara Kannada,
Karnataka

***Abstract*- The present experimental study focuses on the influence of surface roughness and confinement of the jet over the distribution of local wall static pressure and local Nusselt number over a flat plate on impingement by a laminar slot air jet. The major parameters considered in the study are: jet to plate spacing, Reynolds number, Confinement levels of jet etc. The distribution of heat transfer coefficient will be explained in the light of flow behaviour of the jet for given parameters of study. An enhancement in both local wall static pressure and Nusselt number values are expected particularly in the potential core and stagnation regions of the jet.**

Key words:Jet to plate spacing (Z/D_h), Reynolds Number (Re), Confinement ratio (L_c/D_h), Stagnation region, Nusselt Number (Nu), Coefficient of wall static pressure (C_p).

1. INTRODUCTION

Impinging jets are used in a wide range of industrial processes as an efficient means to enhance and control localized heat and mass transfer. Applications of impinging jets include drying of textiles, film, and paper; cooling of gas turbine components and the outer wall of combustors; freezing of tissue in cryosurgery; and cooling of electronic equipment. Significant attention has been paid to impinging.

The impinging jets can be classified by their boundary as confined or unconfined flow field. The unconfined geometries were frequently used in the earlier studies on impinging jets. Confined geometry, where the radial spread of the jet is bounded by a confinement plate, has been investigated extensively in literature due to its importance in industrial applications.

The most important difference between unconfined and confined jets, that affects the flow field and subsequently heat transfer characteristics, is the entrainment of surrounding air.

Zhou and Lee [1] studied the heat transfer and fluid flow characteristics of rectangular jet impinging on a heated plate. They experimentally studied the effect of Reynolds number and nozzle to plate spacing on local and average Nusselt number. They observed that higher Reynolds number produces larger mean velocity and turbulence intensity. They were also observed that nozzle to plate spacing has more significant influence on heat transfer of impingement region. They reported a correlation relating local and average Nusselt number and free stream turbulence. Narayan et al [2] experimentally studied the flow field surface pressure and heat transfer of turbulent slot jet. Two nozzle to surface spacing at 3.5 (transitional jet) and 0.5 (potential core jets) nozzle exit hydraulic diameter are considered for exist Reynolds number at 23000. They reported high heat transfer rate in the transitional jet impingement and non-monotonic decay in heat transfer coefficient. Katti and Prabhu [3] studied enhancement of heat transfer on a flat plate surface using axis symmetrical ribs by normal impingement of circular jet. Effect of ribs width (w) ribs height (e) pitch between the ribs (p) location of first rib from stagnation point and clearance under the rib (c) on local heat transfer distribution is studied jet to plate distance varying from 0.5 to 0.6. They observed that the enhancement in heat transfer due to acceleration of fluid in that region created by clearance under the rib and Nusselt number of stagnation point increases by shifting rib nearer to the stagnation. They also observed wall static pressure gradient of stagnation point is higher for surface with detached ribs than smooth surface. Katti et.al [4] experimentally studied the local wall static pressure distribution on smooth and rough surface by impinging slot jet. They observed that wall static pressure is independent of Reynolds number and its strength decreases with increase in nozzle to plate spacing, they also observed enhancement in heat transfer rate at rough surface using detached ribs compare to smooth surface. Nirmalkumar et al [5] conducted experimental investigation of local heat transfer distribution and fluid flow properties on a smooth plate by impinging slot air jet. Reynolds number based on slot width varied from 0.5 to 12. They identified three regimes on the flat surface viz. stagnation region ($0 \leq x \leq 2$), transition

International Journal of Engineering Research & Technology (IJERT)
ISSN: 2278-0181
Vol. 5 Issue 06, June-2016

region ($2 \leq x/b \leq 5$) and wall jet region ($x/b \geq 5$). Semi empirical correlation for Nusselt number in the stagnation region and wall jet region is suggested and similar work is carried out by Adimurthy *et al* [6]. Gau and Lee [7] studied fluid flow and heat transfer along the triangular rib roughened wall by impingement of slot air jet. The effect of rib heights on fluid flow and heat transfer along the wall is studied. They observed that widely opened cavity between neighbouring ribs make more intense transport of momentum between the wall jet and cavity flow that leads to higher heat transfer rate and in the region of laminar wall jet that leads to reduction in heat transfer. The correlation of stagnation Nusselt number presented. Chao and Kim [8] compared the thermal characteristics of confined and unconfined impinging jets. The effect of pumping power and flow rate studied by varying Reynolds number from 3600 to 17300 and two nozzle to plate spacing of 0.125 and 0.25. They observed the thermal characteristics of confined jet is similar to unconfined jet of fixed pumping power condition while thermal performance of confined is 20% to 30% lower than unconfined jet under fixed flow condition. Puneet Gulati et al [9] studied the effects of shape of nozzle, jet to plate spacing and Reynolds number on impinging air jet. Reynolds number varied between 5000 to 15000 and jet to plate spacing from 0.5 to 12 Nozzle diameters. Length to equivalent diameter ratio of 50 is chosen. They observed that rectangular nozzles show high heat transfer rate due to high turbulence intensity at nozzle exit. Beitelmal et al [10] studied the effect of surface roughness on average heat transfer at on impinging air jet. The temperature was measured over a Reynolds number ranging from 9600 to 38500.Nozzle to plate spacing (z/d) ranging from 1 to 10. They observed up to 6%increase in average Nusselt number due to surface roughness that disturbs the boundary layer and promotes the turbulence of wall jet. The correlation between average Nusselt number, Reynolds number and nozzle to plate spacing was proposed. Gardon and Akfirat [11] studied the effect of velocity and turbulence on heat transfer characteristics of impinging two dimensional jets by varying Reynolds number from 450 to 22000 and slot width of 1.58, 3.175 and 6.35 mm. the observed non monotonic variation of heat transfer along stream wise direction. Stagnation point Nusselt number is to be constant for nozzle to placing below the length of potential core. They also observed heat transfer of laminar boundary layer with positive pressure gradient is more than turbulent boundary layer is observed at pressure gradient. They reported that stagnation Nusselt number is higher at jet impinging on target plate at end of potential core.

The objective of this investigation is to examine the effects of geometric parameters on wall static pressure distribution and heat transfer of the impinging jet on a confined rough surface. The parameters included in the study are: nozzle-to-plate spacing (Z/D_h), Reynolds number, confinement ratio and target plate roughness. A relationship between stagnation Nusselt number (Nu_0) and nozzle to plate spacing (Z/D_h) is proposed using graphical curve fitting method.

2. EXPERIMENTAL SETUP

The experimental set-up for wall static pressure distribution and heat transfer studies are as shown in Figure.1 Air is supplied by a blower through a calibrated orifice meter. The flow rate is controlled by a flow control valve. To achieve the uniform flow rate at the exit of the nozzle, the airflow is

NOMENCLATURE

A	Surface area of the smooth surface, m^2	Nu_0	Local Nusselt number at stagnation point, W/m^2K
A_j	Area of jet, m^2	Q	Heater input power , W
D_h	Hydraulic diameter of the jet ,m	q	Heat flux , W/m^2
B	Width of the nozzle, m	Re_j	Reynolds number of jet
H	Height of nozzle, m	Ta	Ambient air temperature , K
Q_{act}	Actual discharge of air, m^3/s	Tj	Jet temperature at nozzle exit, K
C_d	Coefficient of discharge	Tw	Target plate surface temperature, K
C_p	Coefficient of wall static pressure	V	Voltage , volt
h	Heat transfer co-efficient , W/m^2 K	v_j	Jet velocity at nozzle exit , m/s
I	Current, Amp	Z	Nozzle to plate spacing, m
k	Thermal conductivity of the jet fluid, W/m K	L_c/D_h	Confinement ratio.
Nu	Local Nusselt number, W/m^2K	Z/D_h	Dimensionless distance between nozzle exit and target plate

directed to the plenum through a diffuser and two meshes in the plenum. Velocity profile remains uniform because of the diffuser upstream of the plenum. Nozzle is made of an acrylic sheet with 45 mm height and 4 mm wide. The aspect ratio of the nozzle cross section is maintained very high around 24 so that the effect of nozzle height is neglected. Jet air temperature is measured using a Chromel-AlumelThermocouple (K-type) positioned at the inlet of the nozzle. For smooth surface flow study the target plate which is made up of acrylic sheet of 10mm thickness. A static pressure tap

International Journal of Engineering Research & Technology (IJERT)
ISSN: 2278-0181
Vol. 5 Issue 06, June-2016

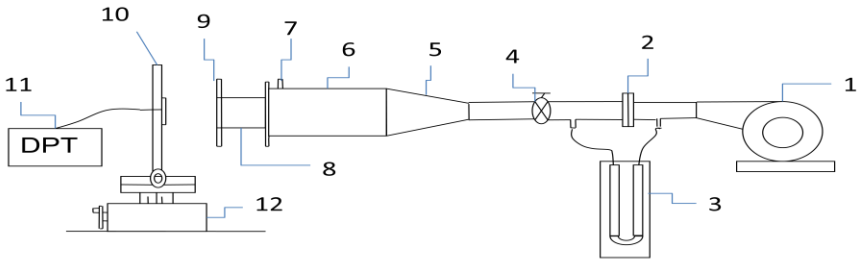

1.Air blower, 2. Orifice meter, 3.U-tube manometer, 4.Control valve, 5.Diffuser, 6.Plenum , 7.Thermocouple, 8.Nozzle, 9.Confinement plate, 10.Ribbed target plate, 11.Differential pressure transmitter, 12.2D Transverse table

Fig. 1. Experimental set up for wall static pressure measurement

approximately 0.5mm in diameter is drilled in 10mm thick acrylic plate for 3mm deep from impingement surface and then counter bored to 3mm diameter for the remaining depth. The target plate assembly is mounted on a 2-D traverse so that the nozzle to plate distances required can be easily adjusted. The jet-to-plate distances (Z/D_h) of 0.5, 1.0, 2.0, 4.0, 6.0, 8.0, and 10 are considered in the present study. Ribbed surface flow study is done on the same target plate with detached ribs. The ribs are fabricated from the thermally non active material Plexiglas (K=0.23w/mk). Two ribs of size 4mm and 6mm width, 45mm height and thickness is 2mm are chosen for the study. The spacer of thickness 1mm is used to mount the rib over the target plate to maintain uniform gap between the plate and the rib.

To conduct the flow study experiment it is necessary to check all the devices proper connection used in the set up. Cold junction is made by inserting the thermocouple bead in the mercury-water interface place in the thermos flask containing ice -water interface. Before switching on the blower the initial adjustment of jet to plate spacing is set using 2-D traverse table. Initial position of water in the water column manometer is noted and set at equal position. To measure the wall static pressure on the target plate, the static pressure tap is connected to the Differential Pressure (DP) transmitter. Air is supplied by a blower through a calibrated orifice. The required flow rate is adjusted by using the flow control valves to maintain the required Reynolds number. The difference in the two limbs of the column gives pressure drop across flow meter. The blower supplies the air through calibrated flow meters to get the required range of Reynolds number at the exit of the jet. The air is directed to plenum chamber through a diffuser; it is an attachment or duct for broadening airflow and reducing its speed. The plenum chamber is provided with two screens made of fine wire mesh and acts as a flow straightner. At the exit of the plenum chamber the slot jet is mounted. While the jet impinges on the target plate the pressure along the plate is measured using DP, in the stream wise direction by moving the pressure tap in steps of 1mm distance on both sides from the stagnation point and the data is recorded. The jet exit temperature is measured using milli volt meter for every position. The procedure is repeated with different jet to plate spacing's considered in the study. The entire experiment is repeated after mounting the ribs and confinement plate of various dimensions to study the flow behaviour over a rough surface. The ribs and spacers are fabricated from the thermally non active Plexiglas material. Spacers of 1mm thickness are attached to the rib and the rib is mounted on the target plate using Ana bond adhesive. The experiment is conducted for different jet to plate spacing (Z/D_h = 0.5, 1.2. 4, 6, 8, 10) and for a Reynolds number 2500 chosen. The heat transfer study is also conducted on the same set up, by replacing the target plate with a target plate cum heater made of stainless steel foil of size 100mm x 74mm x 0.06mm is clamped tightly and stretched between copper bus bars. To conduct the experiment the target plate is heated by supplying the power through a regulated DC power supply. The I.R Camera is placed back of the target plate on the 2-D traversing table. The I.R Camera is positioned such that to capture the image of the target plate. The target plate is heated to sufficient temperature level (at least 150 above the jet temperature). Then the required jet to plate spacing (Z/D_h) is adjusted using traversing table. After adjusting the all parameters the target plate has to be heated until it attains the stable temperature and the IR image is captured. The Infra red thermal imager is provided with a smart view which is the powerful, easy to use, analysis reporting software. Smart view, together with the thermal imager, enables to: Transfer thermo-graphic images to a computer and manage them. The experiment is repeated with different confinements and a target plate mounted with the ribs to provide the surface roughness.

International Journal of Engineering Research & Technology (IJERT)
ISSN: 2278-0181
Vol. 5 Issue 06, June-2016

3. DATA REDUCTION

Digitization of thermal images for temperature distribution on impingement surface is carried out by SMART VIEW software. The temperature distribution on the flat plate is estimated by averaging the thermal images obtained for each configuration.

Co-efficient of wall static pressure calculated by

$$C_p = \frac{2\Delta p}{\rho_a V_j^2} \quad \text{.....(1)}$$

$$V_j = \frac{Q_{act}}{A_j} \quad \text{.....(2)}$$

$$Q_{act} = C_d \left[\frac{a_1 \times a_2 \sqrt{2gh}}{\sqrt{(a_1^2 - a_2^2)}} \right] \quad \text{.....(3)}$$

Nusselt number calculated by

$$Nu = \frac{h \times D_h}{k} \quad \text{.....(4)}$$

$$h = \frac{q_{conv}}{(T_w - T_j)} \quad \text{.....(5)}$$

The convective heat transfer between impinging jet and target plate is estimated as follows:

$$q_{conv} = q_{joule} - q_{loss} \quad \text{.....(6)}$$

$$q_{joule} = \frac{V \times I}{A} \quad \text{.....(7)}$$

$$q_{loss} = q_{rad(f)} + q_{rad(b)} + q_{nat} \quad \text{.....(8)}$$

q_{loss} is estimated experimentally

Uncertainties in measurement of wall static pressure coefficient and heat transfer coefficients are carried out using method suggested by Moffat [12]. Uncertainty in wall static pressure and heat transfer is 6.5% and 5% respectively.

4. RESULTS AND DISCUSSION

Experiments are carried out to find the wall static pressure and heat transfer distribution of detached ribbed surface along with confinement for Reynolds number 2500, rib width of 4mm and 6mm and confinement ratios of 6.8, 10.2 and 13.6.

4.1 Local wall static pressure distribution

Fig. 2(a-c) shows local wall static pressure distribution along stream wise direction for nozzle to plate spacing's of 0.5, 1.0, 2.0, 4.0, 6.0, 8.0 and 10.0 at Reynolds number 2500 of 4mm rib width along with 6.8, 10.2 and 13.6 confinement ratio. The wall static pressure decreases rapidly at x/D_h = 0.13 – 0.4 due to vena contract in orifice jets [1].

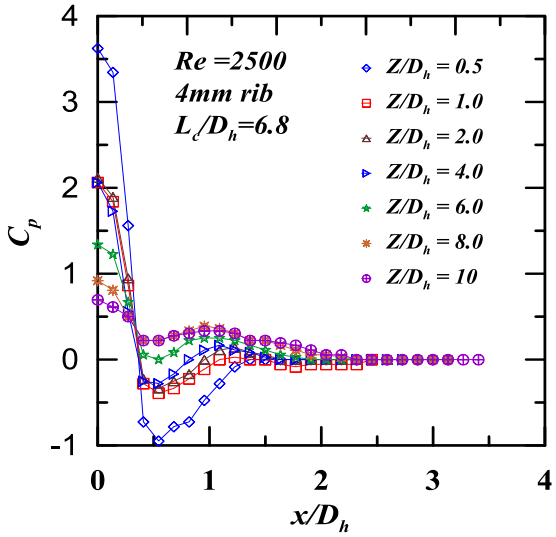

Fig. 2(a)

The local wall static pressure is decreases along the stream wise direction with increase in nozzle to plate spacing. Maximum stagnation wall static pressure occurred at Z/D_h=0.5 for 4mm rib and 6.8 confinement ratio. Due to placing of detached rib and confinement the sub atmospheric region is pronounced up to end of potential core region. The strength of potential core region high at lower nozzle to plate spacing (Z/D_h=0.5) for all confinement ratios studied, sub atmospheric region occurred at x/D_h=0.4. With increase in confinement ratio the strength of sub atmospheric region is decreased and maximum value of C_p is occurred at x/D_h=0.544 that is at end of rib because flow acceleration between the plate and rib at end of rib that cause least value of pressure in sub atmospheric region.

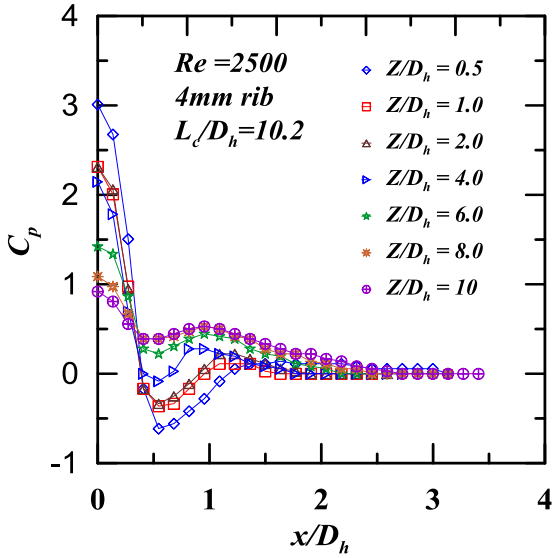

Fig. 2(b)

Secondary peaks in wall static pressure observed for all nozzle to plate spacing of 10.2 confinement ratio and except Z/D_h=0.5 for 6.8 and except Z/D_h=0.5 to 1.0 for 13.6 confinement ratio. The strength of secondary peaks increase with increase in nozzle to plate spacing and maximum value of C_p in secondary peaks occurred at Z/D_h=10 for 6.8 and 10.2 confinement ratio and Z/D_h=8.0 for 13.6 confinement ratio.

International Journal of Engineering Research & Technology (IJERT)
ISSN: 2278-0181
Vol. 5 Issue 06, June-2016

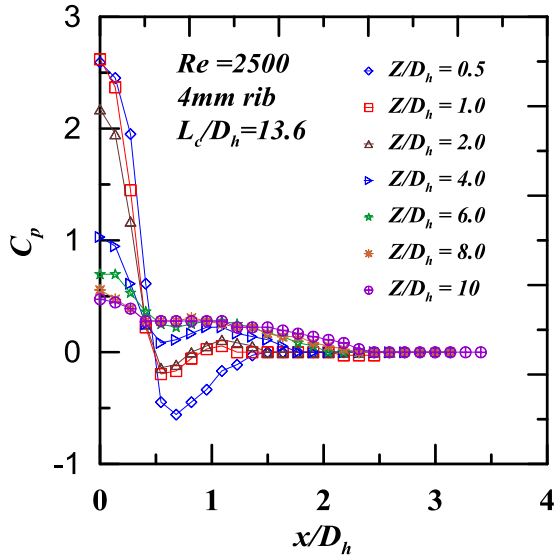

Fig. 2(c)

Fig. 2(a-c). Variation of Wall static pressure in stream wise direction for different nozzle to plate spacing of 4mm rib with different configuration ratio

The wall jet region (Zero pressure gradients) occurred at lower x/D_h values for lower Z/D_h values and wall jet region initiation point move away from centreline of jet with increase in nozzle to plate spacing due increase spreading of jet by entraining the surrounding air. Comparing all confinement ratios the 10.2 confinement ratio shows better stagnation wall static pressure, high strength of sub atmospheric and secondary peaks for all Z/D_h values.

Fig. 3(a-c) shows variation of local wall static pressure along stream wise direction with nozzle to plate spacing's of 6mm rib of different confinement ratio. The maximum stagnation wall static pressure occurred at centreline of jet at Z/D_h=0.5 for all confinement ratio, decreases with increase in nozzle to plate spacing's.

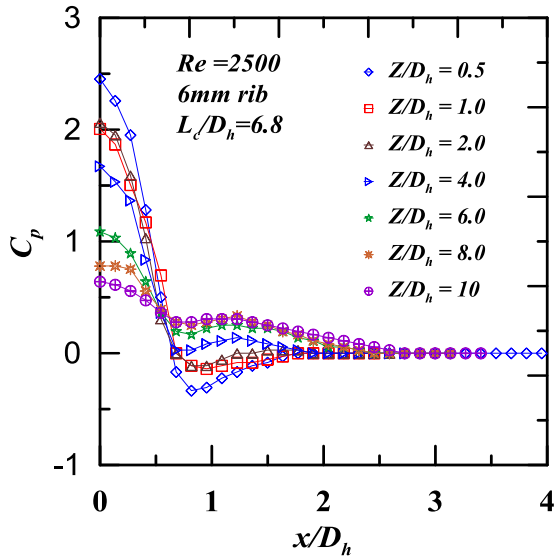

Fig. 3(a)

The sub atmospheric region occurs up to end of potential core region (Z/D_h=4.0) from x/D_h=0.68 at end of rib. The strength of sub atmospheric region decrease with increase in nozzle to plate spacing.

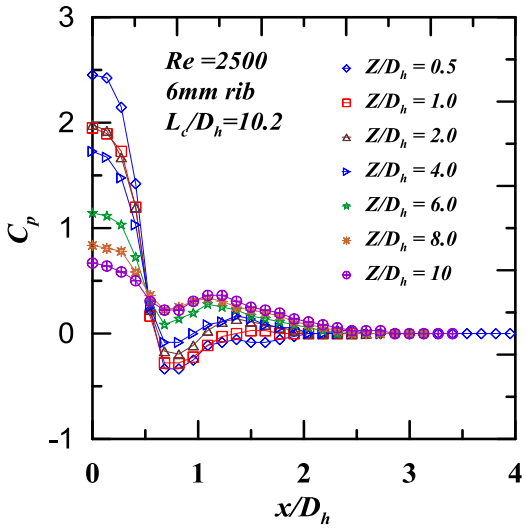

Fig. 3(b)

The secondary peaks in wall static pressure is observed for all Z/D_h values of 10.2 confinement ratio and from Z/D_h=2.0 for 6.8 and 13.6 confinement ratios and its strength increase with increase in Z/D_h value.

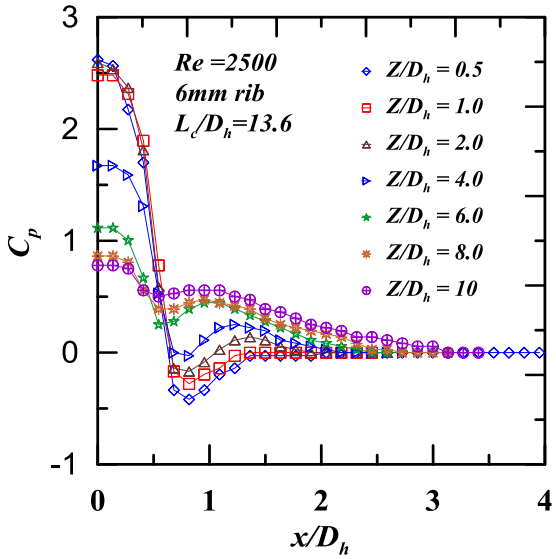

Fig. 3(c)

Fig. 3(a-c). Variation of wall static pressure along stream wise direction for different nozzle to plate spacing of 6mm rib of different confinement ratio.

Comparing all confinement ratios the 10.2 confinement ratio shows better results.

International Journal of Engineering Research & Technology (IJERT)
ISSN: 2278-0181
Vol. 5 Issue 06, June-2016

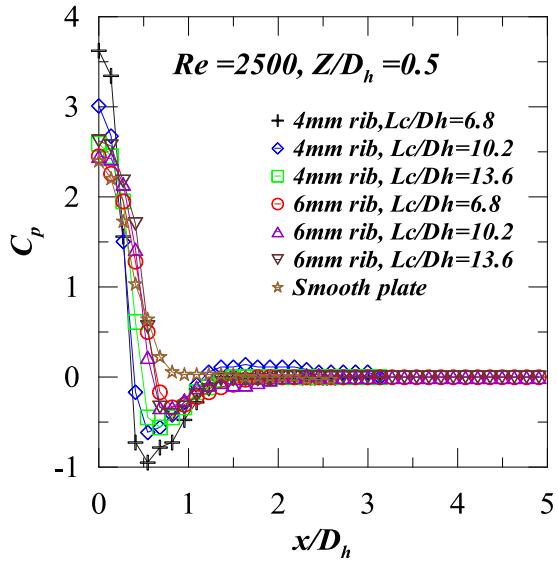

Fig. 4(a)

Fig. 4(a-e) compares variation of a wall static pressure along stream wise direction for different rib and confinement ratio with unconfined smooth surface. The 4mm rib shows better increment in stagnation, sub atmospheric and secondary peaks of wall static pressure for all confinement ratios compare to 6mm rib because with increasing in width of rib major flow impinges on top surface of rib and may not reach to target surface it may lead to decrease in wall static pressure. Wall static pressure gradient of stagnation point is higher for surface with detached ribs than smooth surface [3].

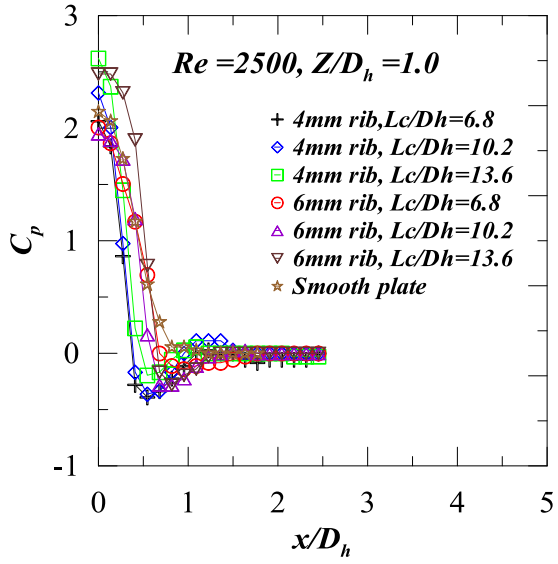

Fig. 4(b)

Comparing to smooth surface confined ribbed surface produces sub atmospheric region in potential core zone and secondary peaks in after potential core zone.

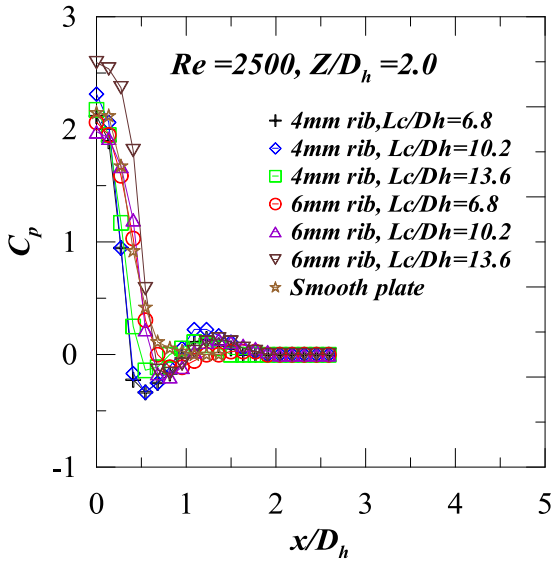

Fig. 4(c)

Sub atmospheric region occurred at x/D_h=0.54 for 4mm rib and x/D_h=0.68 for 6mm rib, this indicate that with increase in width of rib sub atmospheric region move away from centre line of jet.

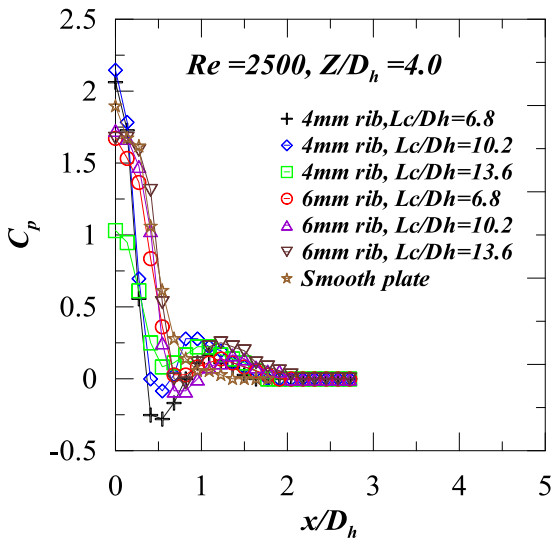

Fig. 4(d)

International Journal of Engineering Research & Technology (IJERT)
ISSN: 2278-0181
Vol. 5 Issue 06, June-2016

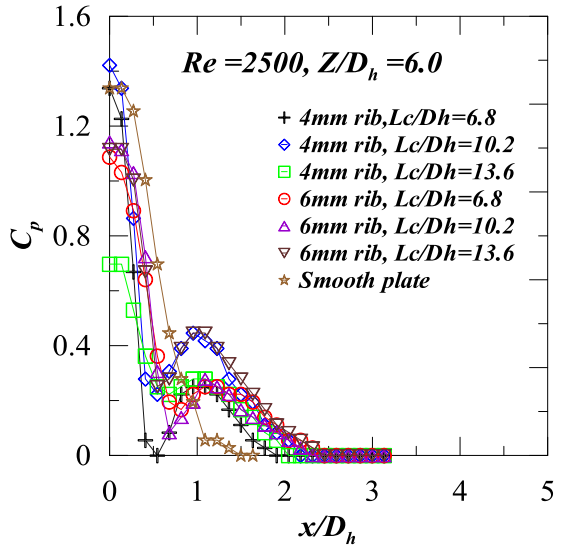

Fig. 4(e)

Fig. 4(a-e). Comparison of wall static pressure along stream wise direction for different rib and confinement ratio.

Fig. 5(a-b) shows the variation of stagnation wall static pressure with nozzle to plate spacing for different confinement ratio of 4mm and 6mm rib.

From Fig. 5(a) there is increases in wall static pressure of 51% for 6.8, 25.5% for 10.2 and 39.5% for 13.6 confinement ratio in comparison with unconfined smooth surface at Z/D_h=0.5 for 4mm rib configuration. The 10.2 and 13.6 confinement ratios shows better results within the potential core region (Z/D_h<4) and 10.2 confinement ratio shows slight higher values of Cp_0 after potential core region.

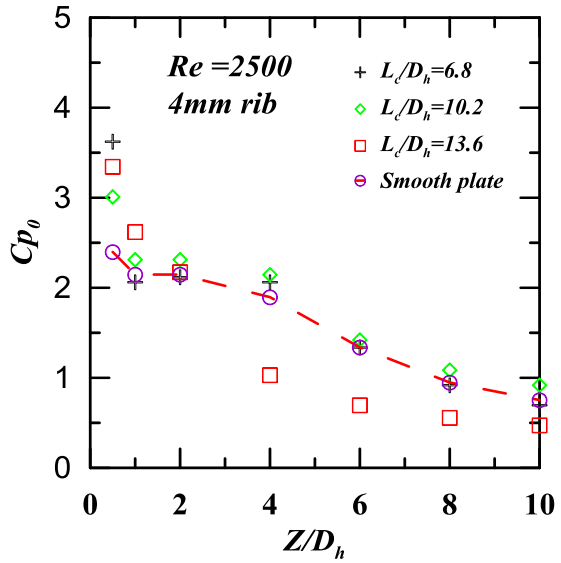

Fig. 5(a)

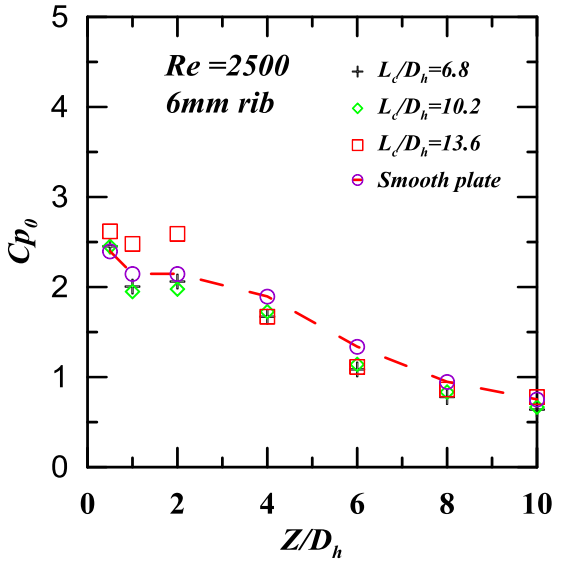

Fig. 5(b)

Fig. 5(a-b). Variation of stagnation wall static pressure with nozzle to plate spacing of different confinement ratio

From Fig. 5(b). Only 13.6 confinement ratio shows better values of Cp_0 within the potential core region, there is increase in Cp_0 9.3% at Z/D_h=0.5, 15.5% at Z/D_h=1.0 and 20.78% at Z/D_h=2.0 compare to smooth surface. After potential core region all confinement ratios shows lower values than smooth surface because, the effect of rib diminishes with increase in width and confinement effect is dominated.

4.2 Local heat transfer distribution

Fig. 6(a-c) shows variation of local Nusselt number along stream wise direction with nozzle to plate spacing of 4mm rib with different confinement ratio. The Nusselt number decreases along stream wise direction with increase with increase in nozzle to plate spacing because spreading of jet may cause decrease in strength of jet. The maximum stagnation Nusselt number occurred at Z/D_h=2.0 for 6.8 and 10.2 confinement ratio and at Z/D_h=4.0 for 13.6 confinement ratio.

International Journal of Engineering Research & Technology (IJERT)
ISSN: 2278-0181
Vol. 5 Issue 06, June-2016

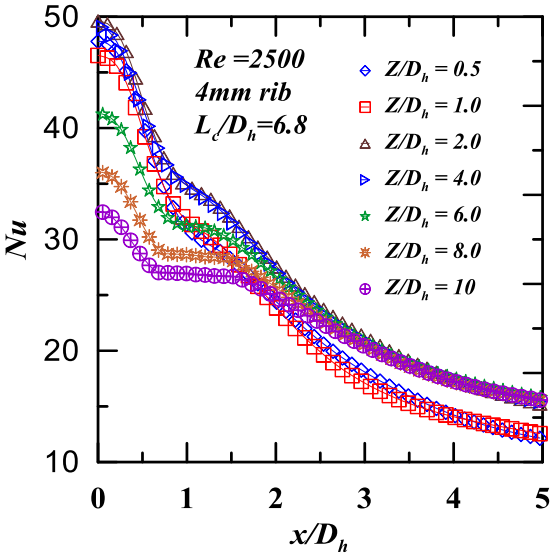

Fig. 6(a)

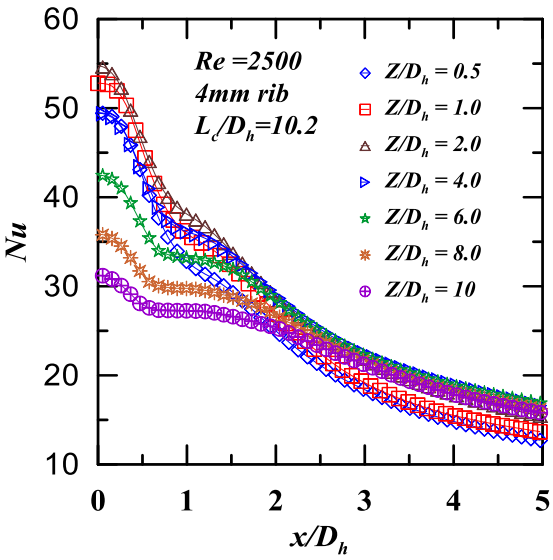

Fig. 6(b)

The secondary peaks in Nusselt number occurred for all nozzle to plate spacing, its visibility increase with Z/D_h values. With increase in confinement the maximum Nusselt number distribution shift to end of potential core region (Z/D_h=4.0) due to increase in turbulence [9].

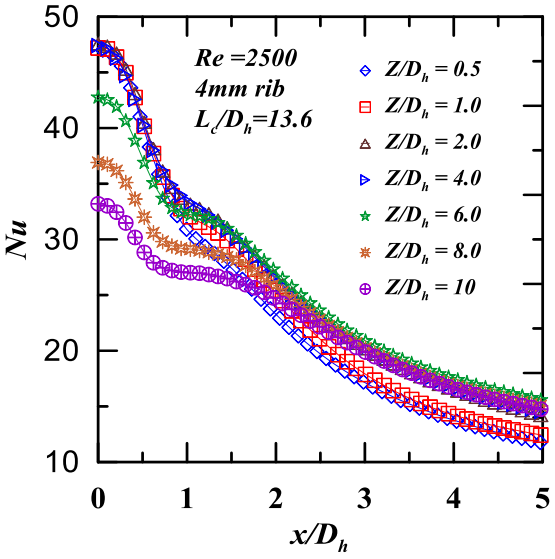

Fig. 6(c)

Fig. 6(a-c) Variation of Nusselt number along stream wise direction for different nozzle to plate spacing of 4mm rib of different confinement ratio.

Fig. 7(a-c) shows variation of local Nusselt number along stream wise direction with nozzle to plate spacing of 6mm rib with different confinement ratios. The Nusselt number decreases monotonically along stream wise direction within potential core region. The secondary peaks observed at Z/D_h>6 for all confinement ratios and maximum stagnation Nusselt number occurred at Z/D_h=4.0 (end of potential core region) for all configurations of 6mm rib.

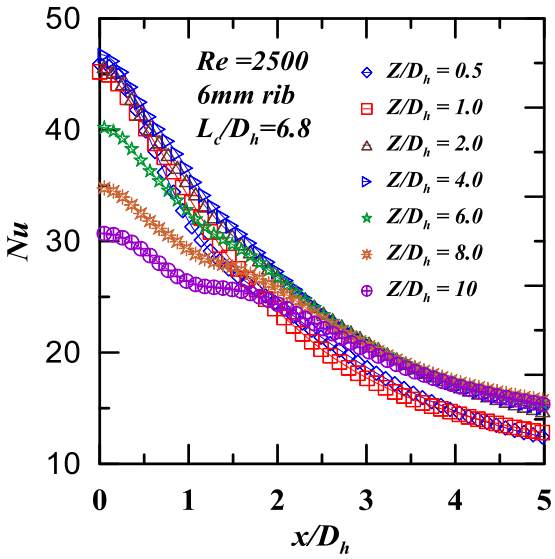

Fig. 7(a)

International Journal of Engineering Research & Technology (IJERT)
ISSN: 2278-0181
Vol. 5 Issue 06, June-2016

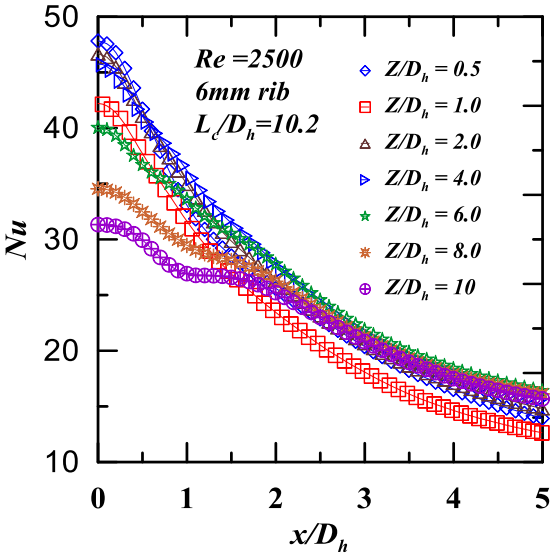

Fig. 7(b)

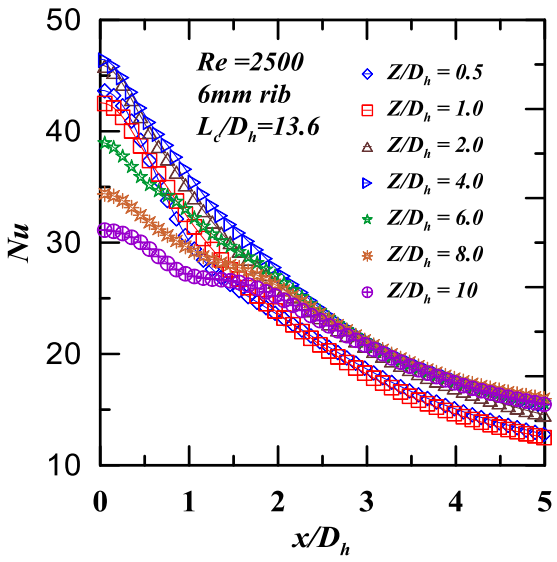

Fig. 7(c)

Fig. 7(a-c) Variation of Nusselt number along the stream wise direction for different nozzle to plate spacing of 6mm rib with different confinement ratio.

Fig. 8(a-b) Shows variation of stagnation Nusselt number with nozzle to plate spacing's of 4mm and 6mm rib with different confinement ratios. From Fig. 8(a) 4mm rib with 10.2 confinement ratio shows better results compare to all configurations and there is augmentation in Nu_0 values of 10.2 confinement ratio,6% at Z/D_h=0.5, 14.5% at Z/D_h=1.0 and 20% at Z/D_h=2.0 compared to unconfined smooth surface. The 13.6 confinement ratio shows higher values of Nu_0 after potential core region.

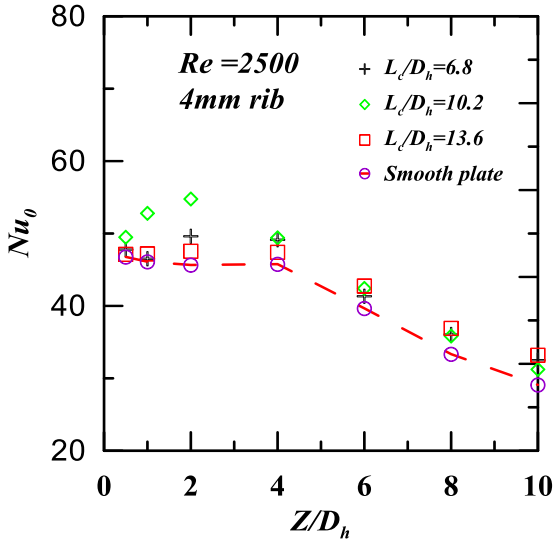

Fig. 8(a)

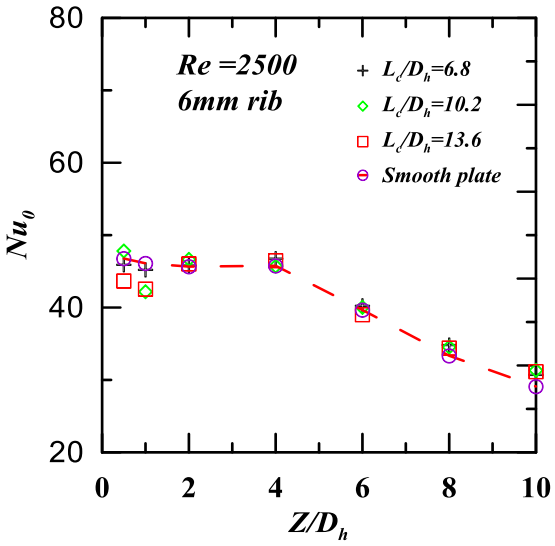

Fig. 8(b)

Fig. 8(a-b) Variation of stagnation Nusselt number with nozzle to plate spacing of different confinement ratio.

From Fig. 8(b) the all configuration shows lower value of Nu_0 compared to smooth surface due to more pronounce of confinement effect with increase in rib width.

4.3 Correlations for stagnation Nusselt number

Correlations for Nu_0, as a function of Z/D_h are developed using the experimental data by curve fitting method. The correlations give the Nu0 values within a maximum deviation of 7.2% in comparison with experimental results.

a) For $0.5 \leq Z/D_h < 4$ (potential core region)

$$Nu_0 = c_1[-3.085(Z/D_h)^2 + 11.23(Z/D_h) + 44.66] \quad ...(9)$$

Where 'c_1 'is correction factor

International Journal of Engineering Research & Technology (IJERT)
ISSN: 2278-0181
Vol. 5 Issue 06, June-2016

Table 4.3.1 Values of c_1

L_c/D_h	6.8	10.2	13.6
4mm rib	0.92	1.0	0.90
6mm rib	0.87	0.65	0.84

b) For $4 \leq Z/D_h \leq 10$ (behind potential core region)

$$Nu_o = c_2\left[-3.055(Z/D_h) + 61.13\right] \text{.....(10)}$$

Table 4.3.2 Values of c_2

L_c/D_h	6.8	10.2	13.6
4mm rib	1.0	1.0	1.01
6mm rib	0.98	0.95	0.95

Maximum deviation is 4.6% compare to experimental results.

5. CONCLUSION

An experimental investigation carried out to study the distribution of local wall static pressure and heat transfer coefficients between the confined slot jet and ribbed rough surface at Reynolds number 2500.

From the study, it is concluded that

Maximum wall static pressure occurs at stagnation point and its value reduces with increase in nozzle to plate spacing for all the configurations investigated.

Sub-atmospheric region is observed up to Z/D_h=4 for all rough surface configurations studied.

Effect of confinement is pronounced more at Z/D_h=0.5 for all configurations since at lower nozzle to plate spacing, more recirculation of the jet happens.

Secondary peaks in wall static pressure are visible invariably at all nozzle to plate spacing and Reynolds number for rough surface due to the effect of flow acceleration under the detached ribs.

Maximum Nusselt number occurs at the stagnation point for all the configurations studied.

4mm rib with confinement ratio 10.2 give better heat transfer coefficient comparatively.

Correlation for stagnation Nusselt number with function of nozzle to plate spacing presented. All correlations give the Nu_0 values within 7.2% deviation.

REFERENCES

[1] Zhou, D. W., and Sang-Joon Lee. "Forced convective heat transfer with impinging rectangular jets." *International Journal of heat and mass transfer* 50.9 (2007): 1916-1926.

[2] Narayanan, V., J. Seyed-Yagoobi, and R. H. Page. "An experimental study of fluid mechanics and heat transfer in an impinging slot jet flow." *International Journal of Heat and Mass Transfer* 47.8 (2004): 1827-1845.

[3] Katti, Vadiraj, and S. V. Prabhu. "Heat transfer enhancement on a flat surface with axisymmetric detached ribs by normal impingement of circular air jet." *International Journal of Heat and Fluid Flow* 29.5 (2008): 1279-1294.

[4] V.V.katti, Adimurthy.M. & Ashwini. .M. Tamagond, "Experimental Investigation on Local Distribution of Wall Static Pressure Coefficient due to Impinging Slot Air Jet on Smooth and Rough Surface". *Journal of Mechanical Engineering Research and Technology*, Volume2, Number 1,(2014)pp500-508.

[5] Nirmalkumar, M., Vadiraj Katti, and S. V. Prabhu. "Local heat transfer distribution on a smooth flat plate impinged by a slot jet." *International journal of heat and mass transfer* 54.1 (2011): 727-738.

[6] M. Adimurtthy, A. P. Ganganavar, V. V. Katti "Local distribution of heat transfer coefficient on a flat plate impinged by a slot air jet". *Proceedings of 40th national conference on Fluid mechanics and Fluid power (fmfp 2013)*

[7] Gau, Chie, and I. C. Lee. "Flow and impingement cooling heat transfer along triangular rib-roughened walls." *International journal of heat and mass transfer* 43.24 (2000): 4405-4418.

[8] Choo, Kyo Sung, and Sung Jin Kim. "Comparison of thermal characteristics of confined and unconfined impinging jets." *International Journal of Heat and Mass Transfer* 53.15 (2010): 3366-3371.

[9] Gulati, Puneet, Vadiraj Katti, and S. V. Prabhu. "Influence of the shape of the nozzle on local heat transfer distribution between smooth flat surface and impinging air jet." *International Journal of Thermal Sciences* 48.3 (2009): 602-617.

[10] Beitelmal, Abdlmonem H., Michel A. Saad, and Chandrakant D. Patel. "Effects of surface roughness on the average heat transfer of an impinging air jet." *International Communications in Heat and Mass Transfer* 27.1 (2000): 1-12

[11] Gardon, Robert, and J. Cahit Akfirat. "The role of turbulence in determining the heat-transfer characteristics of impinging jets." *International Journal of Heat and Mass Transfer* 8.10 (1965): 1261-1272.

[12] R.J. Moffat, Describing the uncertainties in experimental results, Exp.Thermal Fluid Sci. 1 (1988) 3–17.